Immunogenicity of culture filtrated proteins and whole-cell killed formalin of *Listeria monocytogenes* to induced cellular immune response *in vivo*

Hassan H.K. Al-Bayati[1] (iD), Sultan Ahmed Abdullah[1] (iD), Thamer Jaddoa Shihab[1]* (iD), Muthanna Sultan[2] (iD) and Qusai Saleh Jumaa[1] (iD)

[1]*Department of Pathology and Poultry Diseases, College of Veterinary Medicine, University of Tikrit, Tikrit, Iraq*
[2]*Department of Microbiology, College of Veterinary Medicine, University of Tikrit, Tikrit, Iraq*

ABSTRACT

Background: *Listeria monocytogenes* (LM) is a life-threatening bacterium affecting many individuals worldwide, including elderly people, pregnant women, and immune-deficient patients.

Aim: Whole-cell killed formalin of LM antigens (WKLMAgs) and *Listeria* culture filtrated proteins (LCFPs) against challenge-attenuated LM after two booster doses (0 and 14 days) of immunization act as an antigen activating a high level of IgG3, IgM, CXCL2, and IL-1 beta.

Methods: Forty male rats were randomly assigned to four groups. The first group served as a control negative, while the second positive (+) control was inoculation orally 1 ml with virulent (1×10^7 colony forming unit CFU/ml) of LM on day 28, whereas the other two groups were injected with 1-ml WKLMAgs and 1-ml LCFPs in two subcutaneously doses with day 14 intervals, with at day 28 a challenged effective dose (1×10^7 CFU/ml) of virulent LM. Serum blood parameters were measured. During the 35 days, the euthanized animal histopathology studies were performed on the spleen, liver, small intestine, and brain.

Results: The current study indicated a significant difference between *WKLMAgs* and *LCFPs* for serological tests Immunoglobulin (Ig) M, chemokine (C-X-C motif) ligand 2, Ig G3, and interleukin-1 beta compared to both negative and positive controls at *P < 0.001*. Additionally, the *WKLMAgs* and *LCFPs* led to a decrease in the histopathological changes of organs such as (brain, spleen, liver, and intestine) compared to the positive control, which affected the organs with microgranuloma, with a pathological difference between the *WKLMAgs* and *LCFPs* compared to the negative control group.

Conclusion: Both *WKLMAgs* and *LCFPs* are capable to be as a vaccine candidate antigen for the induction of protective immunity against *L. monocytogenes*.

Keywords *L. monocytogenes*, IgM, CXCL2, Vaccine design, PCR.

Introduction

Listeriosis is a disease produced by a Gram-positive bacillus with widespread dissemination in the ecosystem (Mehrannia *et al.*, 2023). It is a predominant food-borne zoonotic disease brought about by *L. monocytogenes* (LM) (Mahmud *et al.*, 2023), which is a contagious and lethal disease of animals, fish, crustaceans, birds, and human beings (Dhama *et al.*, 2015). The disease affects various people, including pregnant women, immune-deficient patients, and elderly people. Listeriosis is categorized by an extensive diversity of diseases separated into dual types, including severe invasive listeriosis, which is characterized by infection of the bloodstream and central nervous system, as well as invading the materno-fetal area (Halbedel *et al.*, 2020; Lachmann *et al.*, 2022) and noninvasive febrile gastroenteritis (Zamuz *et al.*, 2021). By using

actin-based motility, LM can invade and replicate within nonphagocytic cells and spread directly from an infected cell to another cell (Feltham *et al.*, 2024), and to avoid being recognized by the host immune system, listeriolysin-O, the principal virulence factor of LM is essential for controlling the pathogenicity of LM (Cong *et al.*, 2024). LM-induced robust innate immune response and adaptive cellular immune responses (Maudet *et al.*, 2021).

Only two of the 17 identified species in the genus *Listeria*—LM and *L. ivanovii*—are currently considered pathogens. LM is a significant human foodborne microorganism and the third most common source of microbially related foodborne fatalities (Manqele *et al.*, 2023) and is regarded as one of the chief foodborne pathogens for humans globally (Gmeiner *et al.*, 2024). Additionally, LM has also been

well known for inducing abortion in infected pregnant women and cows (Noomy *et al.*, 2021; Mohamed *et al.*, 2022).

Live attenuated vaccines are considered highly recommended, especially *Listeria* associated live vaccine because of their highly immune response and, thus, the virulence. Therefore, the virulence-associated genes and LM virulence are mostly knocked down as a means of virulence reduction (Meng *et al.*, 2020). Culture filtrate proteins (CFPs) from LM act as an effective adjuvant for cellular immunity, and besides, the inactivated whole-cell vaccines provide a full repertoire of antigens to the immune system (Westcott *et al.*, 2023).

The study used serological tests to trace the growth of LM and their activity *in vivo* in research laboratory animals. Interleukin-1 beta (IL-1β), often known as leukocytic pyrogen, is a crucial inflammatory response mediator that also affects various cellular processes, including cell division and proliferation (Bent *et al.*, 2018). Meanwhile, chemokine (C-X-C motif) ligand 2 (CXCL2) is considered a strong neutrophil chemoattractant and is implied in various immune responses (Al-Alwan *et al.*, 2013). However, immunoglobulin G3 (IgG3) is an exceptionally strong Ig that may begin effector processes, for instance, phagocytosis mediated, complement activation by antibodies, or Antibody-dependent cellular cytotoxicity (ADCC) (Damelang *et al.*, 2019). IgM antibodies also offer quick protective immunity and are generated early in the humoral immune response to infections (Fraussen, 2022). In order to reach the goal of vaccine development, the current study aimed to compare between whole-cell killed formalin of LM antigens (*WKLMAgs*) and *Listeria* culture filtrated proteins (*LCFPs*), which clinical trials have not been reported in Iraq yet. Thus, this study has been established to address, investigate, and monitor the immune status of LM in Iraq.

Materials and Methods

Animals used in research
In this research, forty male white Swiss albino rats were used, with an average weight of 110 g and 7 weeks of age. The rats were housed at the animal house of Tikrit's university, the College of Veterinary Medicine. The animal house has been registered and follows the law that the College of Veterinary Medicine legislated under healthy roles and conditions. Free conditions for each rat.

LM Strains
LM was provided by the Medya Diagnostic Center in Erbil, Iraq.

Media preparation
The media were prepared according to the manufacturer's instructions, including heating the constituent, autoclaving, sterilizing for 15 minutes, cooling to 45°C–40°C, and solidifying in Petri dishes.

The culture media were then incubated at 37°C for 24 hours to confirm decontamination for *Listeria* identification agar base (PALCAM) M1064, *Listeria* selective supplement (PALCAM) (FD061), Mac-Conkey agar (MA), and brain heart infusion agar.

Confirmed diagnosis of LM
Polymerase chain reaction (PCR)
PCR (BioRad, USA) procedure is consistent with (Omer *et al.*, 2022). The primer pairs used in the PCR are unique to the *Listeria* species and LM present within the 16S region of the rRNA gene (ABIOpure, USA).

Primers
The primers used are reverse primer 1492-5'-TACGGTTACCTTGTTACGACTT-3' and forward primer 27-5'-AGAGTTTGATCCTGGCTCAG-3', with an annealing temperature set at 60°C. The amplification produces a product of 1,500 base pairs (Promega, USA).

Concentration of DNA
The concentration of DNA is 20 (ng/μl) after extraction from bacteria.

The bacterial identification by Vitek 2 analyzer
Using the automated Vitek 2 Gram-positive analyzer, LM was discovered, confirming the findings of the same organisms' investigation carried out in the ASCO laboratory in Baghdad, Iraq. *Listeria* was completely developed on brain heart infusion agar for 24 hours at around 37°C in the previous test. An examination was performed on 43 biochemical trials estimating the use of sources of carbon, tolerance and inhibition, and enzymatic actions for the programmed documentation of the majority of critical Gram-positive microorganisms. The results for documentation are obtainable in about 9 hours or fewer, consistent with (Crowley *et al.*, 2012).

LM antigens preparation
Whole-cell killed-formalin LM antigens
The brain heart infusion agar from Himedia Company was used to culture LM at 37°C for 24 hours. Intended for immunodominant research, full-grown *Listeria* was collected and centrifuged at 15,000 × g for 15 minutes at 4°C, followed by three rounds of washing in phosphate-buffered saline (PBS). Contrary to cells with 1% formalin residue, it was shaken for 2 hours at 37°C, and then, the cells were incubated at 4°C for 24 hours. After the formalin-killed cells were collected, they were centrifuged at 15,000 × g for 30 minutes at 20°C. The cell pellets were then cleaned with sterile PBS, and the optical density was measured using a spectrophotometer to determine the number of colony-forming units (CFUs) (Luo *et al.*, 2022). The formalin-inactivated cells of sterility test were performed on MA, and for 24 hours at 37°C, the incubation was done (Razzak *et al.*, 2024). These extracts were stored at −80°C until used (Westcott *et al.*, 2023).

LCFPs preparation

Brain heart infusion broth culture was shaken overnight under 37°C. Bacterial cells were then harvested and centrifuged to extract CFP. Then, supernatant was purified by using 0.2-µM minute opening size filters (Tucci *et al.*, 2020). Twenty-four hours later, the sterility test on *Listeria* identification agar base with *Listeria* selective supplement at 37°C, the concentrated CFP was diluted with PBS, and the total protein concentration was assessed by exploitation Bradford's way by Bradford (1976).

Calculating the protein dosage

Based on the evaluation of biochemical protein which was used by Sarkar *et al.* (2024), the complete antigen was identified as a LCFP. The *WKLMAgs* were then normalized by McFarland standards (2) at a cell density of roughly 18 mg/ml (1×10^7 CFU/ml) (Imhof *et al.*, 2023).

Determination challenge dose of LM

The brain heart infusion agar was used to cultivate LM, which was then incubated at 37°C for 24 hours. Four rats were orally infected with 0.2 ml of infectious growth and 0.2 ml of bacterial growth. Rats were watched until the day of the sacrifice. At the time, animals were sacrificed, and slices of liver organs were aseptically removed and cultured on the *Listeria* identification agar base at 37°C for 24 hours (Shalaby *et al.*, 2022). This procedure was repeated until the infected animals died within 24 hours. After dividing the 12 rats into triplet parallel groups, 0.2 cc of bacterial solution contained 1×10^6, 1×10^7, and 1×10^8 CFU/ml of virulent LM individually. Between 24 and 48 hours after inoculation, the number of fatal animals was recorded. The carefully calculated LD50 (1×10^7 CFU/ml) killed 50% of the infected animals (Hardy *et al.*, 2012).

Assembly of blood samples

Blood samples were taken from the retro-orbital plexus vein using a capillary tube after the experimental animals were anesthetized with chloroform. At room temperature, the samples were added to a gel tube and left to coagulate. The next step was to separate the serum by centrifuging the samples at 1,500 rpm for 10 minutes. Following the guidelines of Sunlong Biotech Company, the serum was transferred to an Eppendorf tube and kept at −20°C until needed.

- First, blood draw: On day 0, 2-ml blood was utilized for complete immunological detection.
- Second, blood draws: 2-ml blood was used for (IgM and IL-1 Beta) finding on day 7.
- Third, blood draw: 2-ml blood was used for (IgG-3) finding on day 14.
- Fourth, blood draws: 2-ml blood was used for (CXCL2) finding on day 21.
- Fifth, blood draws: 2-ml blood was used for (IgG-3 and IL-1β) finding on day 28.
- Sixth, blood draw: 2-ml blood was used for (CXCL2 and IgM) finding on day 35.

Study design

In order to clarify and determine the effects of vaccination, an observational study was designed to investigate both immune and pathological effects of LM. In this study, 40 male rats were selected, and they were randomly assigned to four groups, each including 10 male rats according to a protocol authorized by the University of Tikrit Animal Care and Use Committee, which was followed for conducting mouse immunization trials (Kono *et al.*, 2023) and together with the Ma *et al.* (2020). The dosage was established with modifications (Ma *et al.*, 2020).

Group 1

Without inoculation, negative (−) control.

Group 2

Positive (+) control was inoculation orally 1 ml with virulent (1×10^7 CFU/ml) of LM on day 28.

Group 3

Injected with 1-ml *WKLMAgs*, two doses, subcutaneous (S/C) with day 14 intervals for individual rats and at day 28, were inoculated orally with 1-ml challenged effective dose (1×10^7 CFU/ml) of virulent LM.

Group 4

Injected with 1-ml *LCFPs*, two doses, S/C with day 14 intervals for each rat and at day 28, were inoculated orally with 1 ml with a challenged effective dose (1×10^7 CFU/ml) of virulent LM. On the day, 35 animals were euthanized for post-mortem to collect autopsies from the organs (spleen, liver, small intestine, and brain) and then in formalin 10% preservation to the preparation of tissue sections for histopathological examination.

Analysis of serum

Assessment of IgM, IgG-, 3IL-1β, and CXCL2

Rat serum concentrations were measured using the sandwich enzyme-linked immunosorbent assay (ELISA) kit, rat IgM, CXCL2, IL-1β, and IgG3, as per the protocol and instructions provided by the manufacturer. This kit contains a micro-ELISA strip plate that has been pre-coated with an antibody from the anti-serum kit. Standards or samples are added to the appropriate wells of the micro-ELISA strip plate, where they bind to the specific antibody. Following this, the horseradish peroxidase (HRP)-conjugated antibody is introduced to a specific kit and incubated in each well of the micro-ELISA strip plate. The excess ingredients are removed by washing. 3,3′,5,5′-Tetramethylbenzidine, a chromogenic substrate solution, is practical for each well. Individual wells comprising the HRP-conjugated kit Ab and serum kit will be blue at primary and then transformed to yellow when adding the stop solution (Mushtaq *et al.*, 2022).

Histopathological examination

The samples taken from the brain, liver, intestine, and spleen during necropsy were all preserved in a 10% neutral buffered formalin solution. The hematoxylin and eosin staining procedure was then carried out (Al-Sabawi *et al.*, 2023).

Statistical analysis

GraphPad Prism 8 (GraphPad Software, San Diego, CA) was used for statistical analysis. The data were shown as means ± standard error. The normal distribution was complete. Two-way analysis of variance to find any statistically significant differences between the four data groups and Tukey's multiple comparison tests were used to compare the data groupings. (*p < 0.05, **p < 0.01, and ***p <0.001; ns: not significant).

Ethical approval

The animals targeted in this study were housed under pathogen-free conditions in the animal facility at the College of Veterinary Medicine, Tikrit University, according to the ethics and guide No.Tu. Vet.26 (https://2u.pw/W6FOJTsQ).

Results

LM is a zoonotic bacterium, which has the ability to cause severe diseases in both human and animal, including sepsis, neurological disorders, and abortion (Jibo *et al.*, 2022). Andersen and Doherty (2005) reported that numerous CFP antigens have the ability to generate a significant level of protection in animal and human models. For this reason, CFP antigens are a desirable source for novel vaccination and diagnostic tools.

Verification of LM

In order to verify the causative agent, the Vitek 2 analyzer and PCR were both used in the creation of immunogenic materials and ensure that it was not contaminated with other bacteria or biological elements.

Selective media agar by (PALCAM media)

The PALCAM media is a different analytical media that engages two-pointer techniques, such as ferric citrate, esculin, phenol red, and mannitol. The colonies of bacteria formed gray-green marks with a black core and a halo (Fig. 1), due to PALCAM medium proved to be extra selective (p < 0.001) than the modified Oxford (Capita *et al.*, 2001).

The bacterial identification by using the Vitek 2 analyzer

During the period of cultivation, which was 24 hours, the automatic system identified Gram-positive bacteria, which was explainable and displayed 97% upright recognition of LM. Additionally, the existing results validate that the target bacteria strain of LM has the ability to cause the infection (Fig. 2). The result agreed with Kim and his group where they have found that the Vitek 2 analyzer to identify 24 LM isolates from ruminants with listeriosis (Kim *et al.*, 2023).

Identification of LM via PCR

The 16S bacterial rRNA region's 1500-base pair amplicon showed positive amplification in the molecular results in Figure 3, in which out of 100 samples by Bahramian *et al.* (2023). Eleven samples have been recognized as positive for 16S rRNA.

Assay of immunological serum
IgM concentration

IgM antibodies were in charge of the protective effect for both actively and passively generated protection (Salinas-Carmona and Pérez-Rivera, 2004). Recently, an original application viewpoint has investigated the host immune responses toward the extracellular bioactive compounds (CFPs), which produced by the bacteria (Fatsi *et al.*, 2024). *LCFPs* and *WKLMAgs*, which are both produced by the bacteria, can provoke a robust Th1-type immune response, clearance of the bacteria, and resistance to subsequent LM infection (Zenewicz and Shen, 2007; Meng *et al.*, 2020). The IgM gives the impression of substantial alteration (*p < 0.05*) at day 7 in pre-challenge groups of animals G3 and G4 (3408 ± 140.32 and 3305 ± 118.17), respectively, as well at day 35 in post-challenge groups G2–G4 with virulent LM (4084.5 ± 127.16, 2549 ± 162.52, and 2665 ± 134.48) correspondingly, comparison with the G1 control negative (763 ± 23.98 and 696.8 ± 19.17) at days 7 and 35, respectively. However, again, there was no significant difference between G3 and G4 at 7 or 35 days, alongside at day 0 between all groups (769 ± 54.84, 768.5 ± 54.55, 764.7 ± 52.47, and 769.8 ± 53.88), as in Table 1 and Figure 4.

Chemokine (C-X-C motif) ligand 2 (CXCL-2) concentration

The CXCL2 presented significant alteration (*p < 0.05*) at day 21 in pre-challenge groups of animals G3 and G4 (42.52 ± 1.18 and 37.92 ± 7.07), respectively, as well as at day 35 in the post-challenge groups G2–G4 with virulent LM (80.27 ± 1.83, 36.27 ± 4.04,

Fig. 1. Colonies of LM presented on PALCAM agar. Colonies are unable to ferment mannitol or hydrolyze esculin when LM is present. Rather, they have a black halo and a gray-green appearance.

Organism Quantity:
Selected Organism : Listeria monocytogenes

Source: Collected:

Comments:

Identification Information	Analysis Time:	8.00 hours	Status:	Final
Selected Organism	97% Probability	**Listeria monocytogenes**		
	Bionumber:	346200224733621		
ID Analysis Messages	Critical Pathogen, check Camp test and beta-hemolysis			

Biochemical Details

2	AMY	+	4	PIPLC	+	5	dXYL	-	8	ADH1	-	9	BGAL	-	11	AGLU	+
13	APPA	-	14	CDEX	+	15	AspA	+	16	BGAR	-	17	AMAN	+	19	PHOS	-
20	LeuA	(-)	23	ProA	-	24	BGURr	-	25	AGAL	-	26	PyrA	-	27	BGUR	-
28	AlaA	-	29	TyrA	+	30	dSOR	-	31	URE	-	32	POLYB	+	37	dGAL	-
38	dRIB	-	39	ILATk	-	42	LAC	+	44	NAG	+	45	dMAL	+	46	BACI	+
47	NOVO	+	50	NC6.5	+	52	dMAN	-	53	dMNE	+	54	MBdG	+	56	PUL	-
57	dRAF	-	58	O129R	+	59	SAL	+	60	SAC	-	62	dTRE	+	63	ADH2s	-
64	OPTO	+															

Fig. 2. Identification of LM by analyzer VITEK 2 GP card.
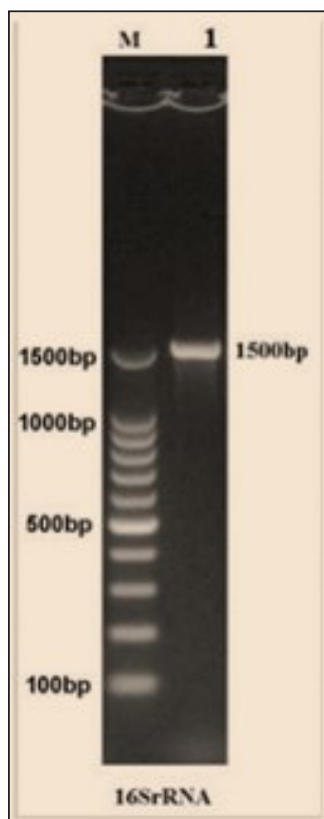

Fig. 3. The final result of the PCR sample. Results of a 1% agarose gel electrophoresis fractionated using an Eth. Br. M: 100 base pairs ladder marker to show the amplification of the 16s RNA gene of an unknown bacterial kind. Lane 1 resembles PCR products consisting of 1500 base pairs.

and 33.68 ± 4.67), in comparison with G1 of control negative (19.22 ± 0.13 and 19.32 ± 0.42) at days 21 and 35. On the other hand, there is no significant difference between G3 and G4 at 21 or 35 days, together with day 0 between all groups (19.15 ± 0.62, 20.07 ± 0.76, 20.91 ± 0.99, and 19.68 ± 1.05) as in Table 2 and Figure 6.

IL-1β concentration

The IL-1β displayed a significant difference ($p < 0.05$) at day 7 in pre-challenge groups of animals G3 and G4 (29.58 ± 0.98 and 27.31 ± 0.88), respectively, in addition at day 28 in the post-challenge with virulent LM groups G2–G4 (52.9 ± 1.78, 24.95 ± 1.05, and 23.77 ± 0.98) separately, in comparison with the control negative G1 that was (10.9 ± 1.57 and 12.7 ± 0.88) at days 7 and 28, respectively. However, no significant difference between G3 and G4 at 7 or 28 days, in common with day 0 among all groups (10.5 ± 0.82, 10.3 ± 1.38, 9.7 ± 0.99, and 8.9 ± 0.9) as in Table 3 and Figure 7.

IgG3 concentration

The IgG3 presented significant alteration ($p < 0.05$) at day 14 in pre-challenge groups of animals G3 and G4 (12.07 ± 0.38 and 11.29 ± 0.48), respectively, as well as after day 28 in the post-challenge groups G2–G4 with virulent LM (12.76 ± 0.79, 6.48 ± 0.57, and 4.43 ± 0.58), respectively, in comparison with the control negative G1 (1.54 ± 0.19 and 1.24 ± 0.25) at days 14 and 28, respectively, but no alteration in day 0 among all groups (1.39 ± 0.43, 1.26 ± 0.26, 1.53 ± 0.18, and 1.45 ± 0.12) as in Table 4 and Figure 7.

Histopathological study

The central nervous system is a specific tropism for LM (Remuzgo-Martĺnez *et al.*, 2013). The control positive

Table 1. The level of immunoglobulin M (mg/ml) in immunized and challenged groups by virulent LM at days 0, 7, and 35 in serum.

Groups	Days (Mean ± SE)		
	0	7	35
G1 = Control negative	769 ± 54.84	763 ± 23.98	696.8 ± 19.17
G2 = Control positive	768.5 ± 54.55	740.3 ± 38.14	4084.5 ± 127.16
G3 = *WKLMAgs*	764.7 ± 52.47	3408 ± 140.32	2549 ± 162.52
G4 = *LCFPs*	769.9 ± 53.88	3305 ± 118.17	2665 ± 134.48

A P-value fewer than 0.05 was well thought-out in addition substantial.
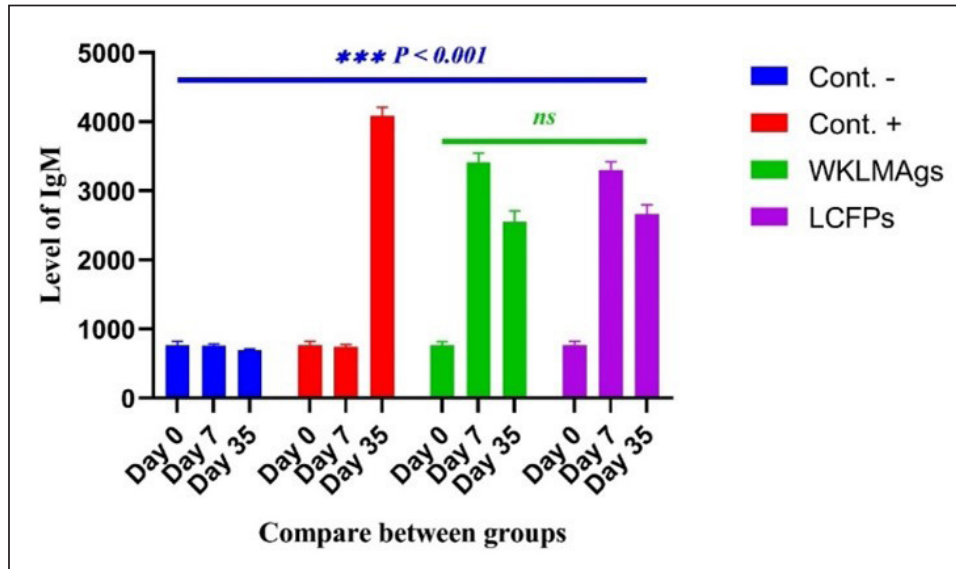
Fig. 4. The pre- and post-challenge statistically significant IgM between the groups demonstrated significant variance *p < 0.001* at day 7 in pre-challenge groups of animals G3 and G4, respectively, as well at day 35 in post-challenge with virulent LM groups G2–G4 correspondingly, compared with the control negative G1. No significant difference between G3 and G4 at 7 or 35 days, alongside at day 0 between all groups. Cont. − = G1, Cont. − = G2, *WKLMAgs* = G3, and *LCFPs* = G4. Two-way ANOVA was used to compare between more than two groups with significant changes in mean total cell (**p* < 0.05, ***p* < 0.01, and ****p* <0.001; ns: not significant).

Table 2. The level of CXCL2 (mg/ml) in immunized and challenged groups by virulent LM at days 0, 21, and 35 in serum.

Groups	Days (Mean ± SE)		
	0	21	35
G1 = Control negative	18.15 ± 0.62	19.22 ± 0.13	19.32 ± 0.42
G2 = Control positive	20.07 ± 0.76	22.49 ± 0.72	80.27 ± 1.83
G3 = *WKLMAgs*	20.91 ± 0.99	42.52 ± 1.18	36.27 ± 4.04
G4 = *LCFPs*	19.68 ± 1.05	37.92 ± 7.07	33.68 ± 4.67

A P-value fewer than 0.05 was well thought-out in addition substantial.

group showed that LM congestive of blood vessels (BVs) with erythrocytes and early polioencephalomalacia, the perivascular accumulation of protein-rich fluid, and minor hemorrhage with micro-abscess resulted in a significant increase in the total number of aggregation inflammatory cells in the ventricles of the brain. *WKLMAgs* and *LCFPs* groups revealed mild injury in brain tissue as a result of encouraging a preventive
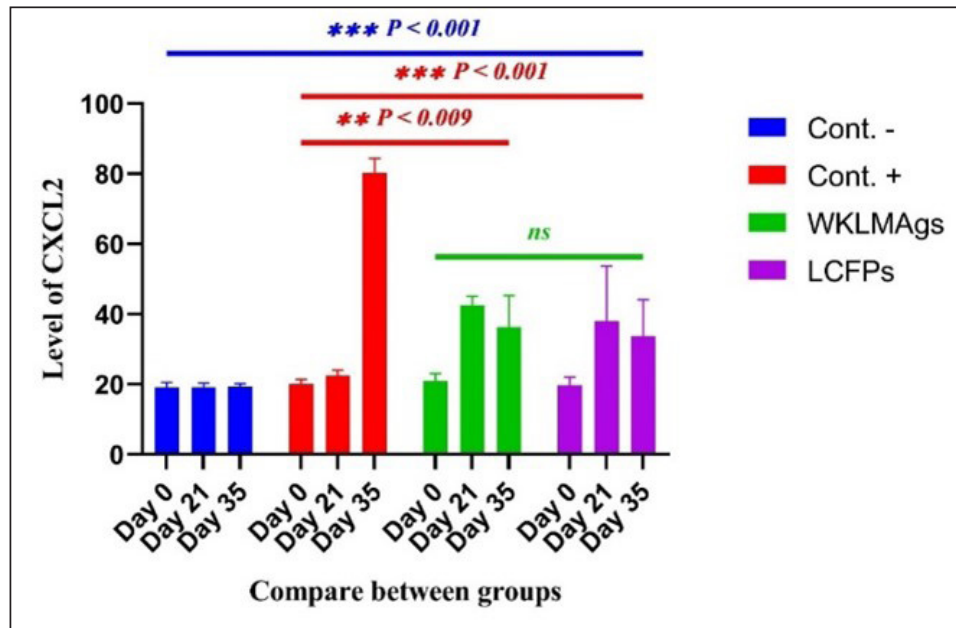
Fig. 6. The pre- and post-challenge statistically substantial IL-1β among the groups presented notable variation $p < 0.001$ and $p < 0.05$ at day 7 in pre-challenge groups of animals G3 and G4, respectively, moreover at day 28 in the post-challenge groups G2–G4 with virulent LM separately, compared with the control negative G1 at days 7 and 28. No substantial difference between G3 and G4 at 7 or 28 days, in common with day 0 among all groups (Cont. − = G1, Cont. − = G2, *WKLMAgs* = G3, and *LCFPs* = G4). Two-way ANOVA was used to evaluate significant changes in mean total cell (*p < 0.05, **p < 0.01, and ***p <0.001; ns: not significant).

Table 3. The level of IL-1β concentration (ng/ml) in the groups of rats challenged with virulent LM and immunized at days 0, 7, and 28 in serum.

Groups	Days (Mean ± SE)		
	0	7	28
G1 = Control negative	10.5 ± 0.82	10.9 ± 1.57	12.7 ± 0.88
G2 = Control positive	10.3 ± 1.38	8.5 ± 0.75	52.9 ± 1.78
G3 = *WKLMAgs*	9.7 ± 0.99	29.58 ± 0.98	24.95 ± 1.05
G4 = *LCFPs*	8.9 ± 0.9	27.31 ± 0.88	23.77 ± 0.98

A P-value fewer than 0.05 was well thought-out in addition substantial.

humoral immune response against intracerebral infection (Sunden *et al.*, 2010) as in Figure 8A, C, and D. However, the groups of *WKLMAgs* showed congestion of BVs in the cortex with nonedematous parenchyma (Fig. 8C), whereas *LCFPs* displayed that the normal structure of the ventricular area of the brain is lined by a simple cuboidal epithelium (SCP) with no periventricular edema in the white pulp (Fig. 8D).

The spleen is made up of white pulp, which contains lymphocytes and lymphatic nodule clusters. Within the lymphatic nodule, there is a germinal center and an off-center central artery. The red pulp surrounds the lymphatic nodules of the white pulp. It consists mostly of venous sinuses and splenic cords (Fig. 9A) in

Cont. −. In contrast, Cont. + showed that the neutrophil polymorphonuclear leukocytes was gathering at sites of infected monocytes in the marginal zone and red pulp, causing necrosis of lymphocytes in the white pulp and congestion (Fig. 9B). However, the section spleen seems lymphoproliferative of the follicle with coalescence, and there is no fibro-hypertrophy of the splenic artery, mild neutrophilic infiltration in the red pulp, and less sinus congestion (Fig. 9C) in *WKLMAgs*. Although the *LCFPs* showed hyperplasia of the lymphoid follicle and coalescence with a germinal center, they contained activated B lymphocytes. The tubular mass of mature T lymphocytes surrounds the central arterioles (Fig. 9D).
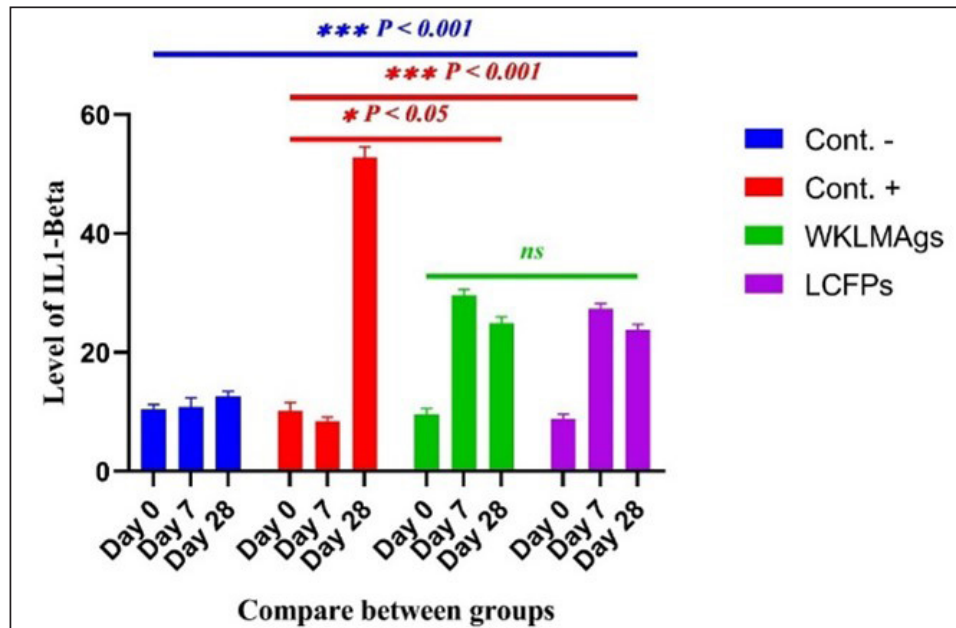
Fig. 7. The pre- and post-challenge statistically significant IgG3 between the groups showing significant change *p* < 0.008 and *p* < 0.001 at day 14 in pre-challenge groups of animals G3 and G4 separately, as well as after day 28 in the post-challenge groups G2–G4 with virulent LM correspondingly, compared with the control negative G1 at days 14 and 28, yet significant difference among G3 and G4 at 7 and 28 days. No alteration on day 0 among all groups (Cont. − = G1, Cont. − = G2, *WKLMAgs* = G3, and *LCFPs* = G4). Two-way ANOVA was used to evaluate significant changes in mean total cell (*p < 0.05, **p < 0.01, and ***p < 0.001; ns: not significant).

Table 4. The Immunoglobulin G3 concentration (ug/ml) at days 0, 14, and 28 in immunized and challenged rats' groups with virulent LM in serum.

Groups	Days (Mean ± SE)		
	0	**14**	**28**
G1 = Control negative	1.39 ± 0.43	1.54 ± 0.19	1.24 ± 0.25
G2 = Control positive	1.26 ± 0.26	1.45 ± 0.12	12.76 ± 0.79
G3 = *WKLMAgs*	1.54 ± 0.19	12.07 ± 0.38	6.48 ± 0.57
G4 = *LCFPs*	1.45 ± 0.12	11.29 ± 0.48	4.43 ± 0.58

A P-value fewer than 0.05 was well thought-out in addition substantial.

The positive control showed microgranuloma, encircled by typical hepatic cell cords, comprised of a buildup of monocytes with congestion (Fig. 10B) differs from (Fig. 10A) of Cont. − = G1 group. However, the hepatic section of *WKLMAgs* appears normal, with organized hepatocytes establishing radiating hepatic cords about the central vein and portal structures, but the hepatic tissues include a slightly dilated blood sinusoid. There were no inflammatory cells in the portal area or the parenchyma, but a proliferation of Kupffer cells (Fig. 10C). Furthermore, the liver shows a central vein at the center of the lobule. Hepatocytes radiate externally from the central vein, split by sinusoidal capillaries and maintained by reticular fibers, with the spread of Kupffer cells in the sinusoids in the *LCFPs* group of Figure 10D as in Figure 10A.

Even though the monocytic cells infiltrated in the submucosa of the small intestine, leading to focal ulcerative enteritis ranging from mild to severe, accompanied by the shedding of mucosal cells into the intestinal lumen in (Fig. 11B) in the Cont. + group. While the lesion of the small intestine in the *WKLMAgs* group shows the absence of aggregations of lymphocyte cells within the lamina propria with an increased number of goblet cells, the planning of intestinal epithelial cells is disordered in Figure 11C comparable in Figure 11A. Furthermore, lesions of the group *LCFPs* appear significant in columnar surface epithelial cells of the
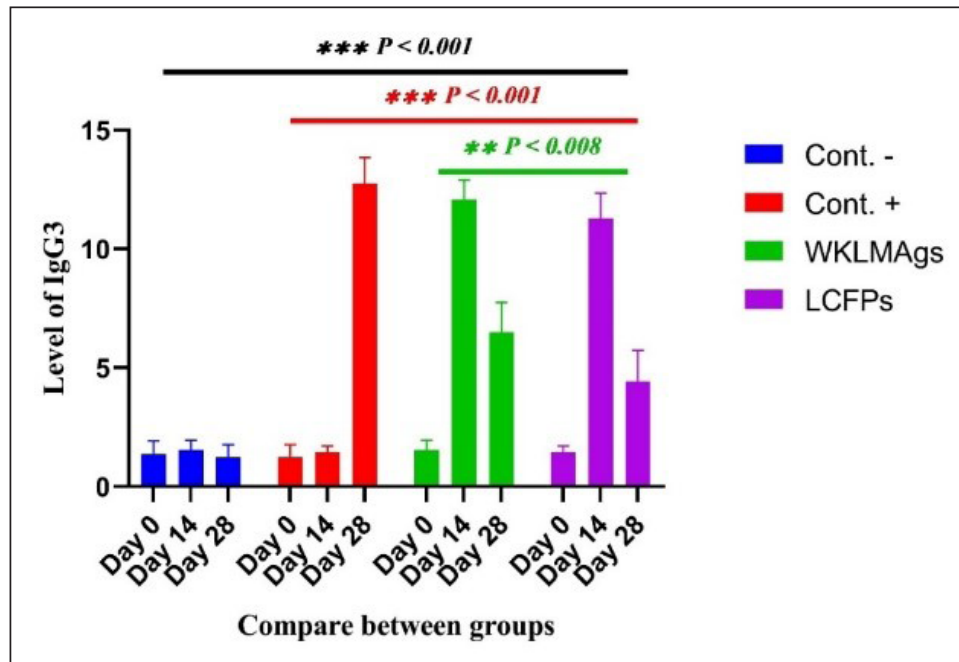
Fig. 8. The H&E staining sections of histopathological brain groups; the section (A) of Cont. − = G1 group showing the pyramidal neurons (A), outer pyramidal cell (B), internal pyramidal cell (C), bigger pyramidal neurons (D), and BVs *X10*. The section (B) of the Cont. + = G2 group viewing the cerebral hemispheres appears congestion of BVs with perivascular edema (E) with hypertrophy of astrocytes (A) and oligodendrocytes (O) *X20*. The section (C) of the *WKLMAgs* = G3 group displays the lesion of the cerebral showing congestion of BVs, with normal structure of cerebral *X20*. The section (D) of the *LCFPs* = G4 group showing the lesion of the cerebral shows the normal structure of ventricular (V) and lined by a SCP and choroid plexus *X10*.

small intestine that are systematized in centers to yield a form of villi, mucin-secreting goblet cells mixed in the epithelium with no aggregation lymphocyte cells in lamina propria (Fig. 11D) analogous in Figure 11A.

Discussion

The majority of natural antibodies are IgM antibodies, which are considered the first class of antibodies to be generated during a primary antibody response against any protein or pathogen (Boes, 2000). Furthermore, class switch recombination occurs after binding to the antigen to express the CD/40 ligand on its surface, which promotes interleukin and cytokine production (Alao *et al.*, 2019). The previous findings on vaccination with whole cells or CFPs that were killed with formalin, which likewise showed the greatest serum antibody titer of IgM, providing strong support for this outcome (Arijo *et al.*, 2004) as this study. In contrast, individuals with IgM deficiency may exhibit clinical some symptoms when they are not asymptomatic, such as invasive or recurring infections, atopy, and autoimmunity (Gupta and Gupta, 2017). Baker *et al.* (2004) demonstrated that for every conjugation, the predominant immune response isotype was IgM with safe and immunogenic in adult health. Additionally, TB

patients' IgM is firmly bound to the protein, and patient sera with anti-HBHA IgM antibodies prevented *M. tuberculosis* from attaching themselves to and invading epithelial cells (Shin *et al.*, 2006), and during the trial, there was no further significant immunostimulant (Table 1 and Fig. 5). While the investigation found a substantial increase in the level of IgM in the control positive groups (4084.5 ± 127.16) compared with G1, G3, and G4, corresponding with (Vernel-Pauillac *et al.*, 2021), as they pointed in their study that mice, which inoculated with the pathogenic bacteria, have maintained high levels of IgM, and compared with other groups G1, G3, and G4 at day 35, reported by Pates *et al.*, (2020) consider the first class of multifunctional, evolutionary conserved antibodies to be created during a primary immune response are called IgM antibodies, which are essential for the early establishment of humoral defense against invasive pathogens. Nevertheless, decreased levels of IgM at day 35 in groups G3 and G4 then induced cellular immune responses (Schaut *et al.*, 2019) and increased the number of long-lasting memory cells, dendritic cells, and macrophages (Beikzadeh, 2024). The results of CXCL2 revealed the high significance of CXCL2 positive control compared to other groups at day 35
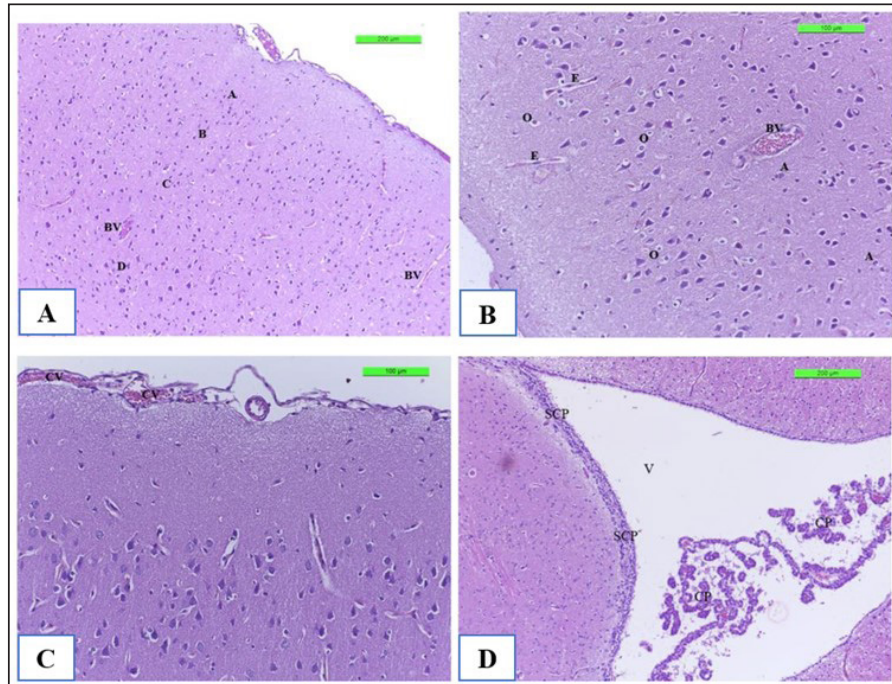
Fig. 9. The H&E staining sections of histopathological spleen groups; the section (A) of Cont. − = G1 group showing a white pulp (WP), germinal center (GC), and red pulp (RP) trabeculae (T) *X10*. The section (B) of Cont. + = G1 group showing small micro-abscess (MA) with multinucleated giant cell (MN) around the focal aggregation of neutrophils in subcapsular region, necrosis (N) with neutrophile infiltration (NI), and hemorrhage (H) *X40*. The section (C) of *WKLMAgs* = G3 group shows the spleen exhibitions lymphoproliferative of follicle (LL) with coalescence (LC), with mild sinus congestion (MSC) *X5*. The section (D) of *WKLMAgs* = G3 group shows the spleen hyperplasia of the lymphoid follicle (HLF), activated B lymphocytes (BC), mature T lymphocytes (TC) around central arterioles (CA) *X5*.

attributable to performance-critical roles in the migration of macrophages, monocytes, and neutrophils (Belperio *et al.*, 2001), which occurs due to neutrophils expressing CXCR1 and CXCR2 chemokine receptors. Moreover, CXCL1 and CXCL2 are considered two of the several chemokine ligands that activate CXCR2. In response to proinflammatory cytokines (Baggiolini, 2001). Both CXCL1 and CXCL2 genes are expressed in the islets of rodents and humans (Cowley *et al.*, 2012). In addition to the peripheral organs targeted by LM (Théroude *et al.*, 2021) as in Figures 9–11B. To be more precise, the vaccination with rCPdA-E first stimulated home macrophages to release chemokines such as CXCL2, which in turn attracted blood neutrophils to the immunization site (Wang *et al.*, 2022). Furthermore, our findings demonstrate at day 21 a decreased level for the *WKLMAgs* and *LCFPs* groups, as a result of the production of CXCL1/2 in the blood, chiefly derived from neutrophils (Biondo *et al.*, 2014) and the formation of Ig from plasma cells after immunization once challenged with *Staphylococcus aureus* or *Salmonella Typhimurium* (Zhou *et al.*, 2022). Similarly, high concentrations of CXCL2 and IL-1β are correlated where the chemokines CXCL1 and CXCL2 are synthesized and secreted in response to IL-1β (Cowley *et al.*, 2012) as in Figure 6. In terms of host defense, a study that has explained the initial line of host defense during the early stages of infection as fish is provided by the classic proinflammatory cytokine genes, such as TNFα and IL-1β, which are crucial in regulating the inflammatory process (Tsai *et al.*, 2014) and here are our findings that were shown of IL-1β appeared significantly at day 7 to be upregulated after immunization by *WKLMAgs* and *LCFPs* since IL-1β is the main controller that regulates systemic responses and other inflammatory stimuli (Pulpipat *et al.*, 2020) and decreases pathological effect as in Figures 8–11C and D and D of G3 and G4. Tahtinen *et al.* (2022) show that RNA vaccines and other inflammatory stimuli can regulate systemic responses by acting as an important regulator of IL-1β and IL-1ra, whereas Prantner *et al.* (2009) and Sahoo *et al.* (2011) indicated that an increased level of IL-1β in positive control because of revealed to be protecting in numerous bacterial, viral, and fungal infections and are essential mediators of cellular immune responses (Van Den Eeckhout *et al.*,
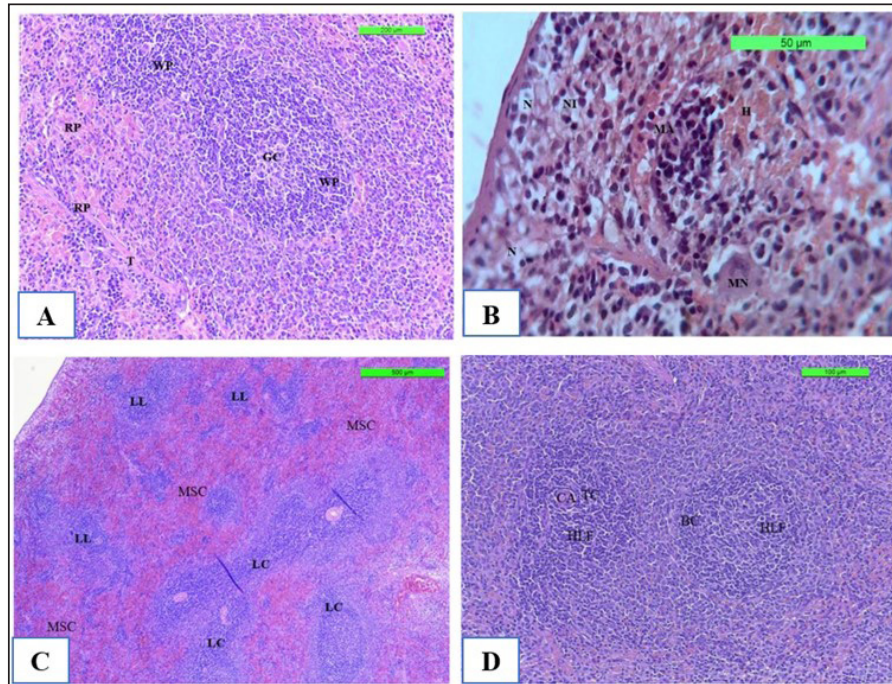
Fig. 10. The H&E staining sections of histopathological groups; the section (A) of Cont. − = G1 group showing central vein (CV), portal area (PA), cords cells (CC), Kupffer cells (KC), and bile canaliculi (BC) *X20*. The section (B) of Cont. + = G1 group displaying liver congestion of central vein (CC), a small micro-abscess (MA) around the central vein with proliferation of Kupffer cells in sinusoids, swelling of hepatocyte (SH) *X10*. Section (C) of *WKLMAgs* = G3 group reveals normal organization of liver hepatocytes (NH) around the central vein and portal structures, slightly dilated blood sinusoid (SD), and proliferation of Kupffer cells (K) *X20*. The section of *LCFPs* = G4 group appears normal radiated of hepatocytes of the liver (NH) around the central vein and portal structures, proliferation of Kupffer cells (K) *X20*.

2020), as well as IL-1β plays an important role in attracting immune cells to the site of infection (Figs. 9 and 10B) (Silvério *et al.*, 2021). Similarly, after 24 hours of vaccination, the spleen's production of the IL-1β gene steadily increased and peaked at more than 72 hours (Pulpipat *et al.*, 2020). Additionally, IL-1β prevents sepsis by promoting local BMC proliferation and differentiation into CD11c−CD45RBhigh DCs at both immunological and nonimmune organs in mouse models (Guo *et al.*, 2021). Moreover, intragastric vaccination with heat-killed *Salmonella enterica serovar Enteritidis* (SE) and IL-1β-secreting *lactobacilli* led to strong SE-specific antibody generation (Kajikawa *et al.*, 2010) as in Figures 4 and 7. Lentini *et al.* (2022) said that the formylated peptide (Fpr) receptors and TLRs are both simultaneously activated when neutrophils encounter live, but not dead, bacteria, which resulted in the production of large concentrations of CXCL2. Napodano *et al.* (2021) demonstrated that the IgG3 antibody is a subclass of the IgG antibody, which ingests pathogens by phagocytic cells by adhering to the pathogen with the antibody's Fab end and to the phagocytic cell's surface via Fc receptors. It aids phagocytosis and bridges the bacterium and the phagocytic cell (Napodano *et al.*, 2021), demonstrated by the lack of substantial change in the tissues of the experimental animals in the histopathological investigation of the third and fourth groups as a result of antibodies binding to vaccination proteins. As discussed by Vidarsson et al. (2014) the various subclasses have distinct effector activities, both in terms of activating complement and triggering cells that express FcγR, which can lead to phagocytosis or antibody-dependent cell-mediated cytotoxicity. These findings enable them to guard against malaria via complement-mediated lysis (Boyle *et al.*, 2015) and cell-mediated processes such as opsonic phagocytosis (Kana *et al.*, 2019) and antibody-dependent cellular inhibition during post-challenge with virulent LM (Oeuvray *et al.*, 1994). It was observed by Genel and Kutukculer (2003) that patients with IgG subclass deficit may have difficulty manufacturing particular antibodies. In a previous study, vaccination failures (insufficient production of specific antibodies in IgG form) against tetanus were 12.3% and 2.7%, respectively, in individuals with isolated IgG subclass
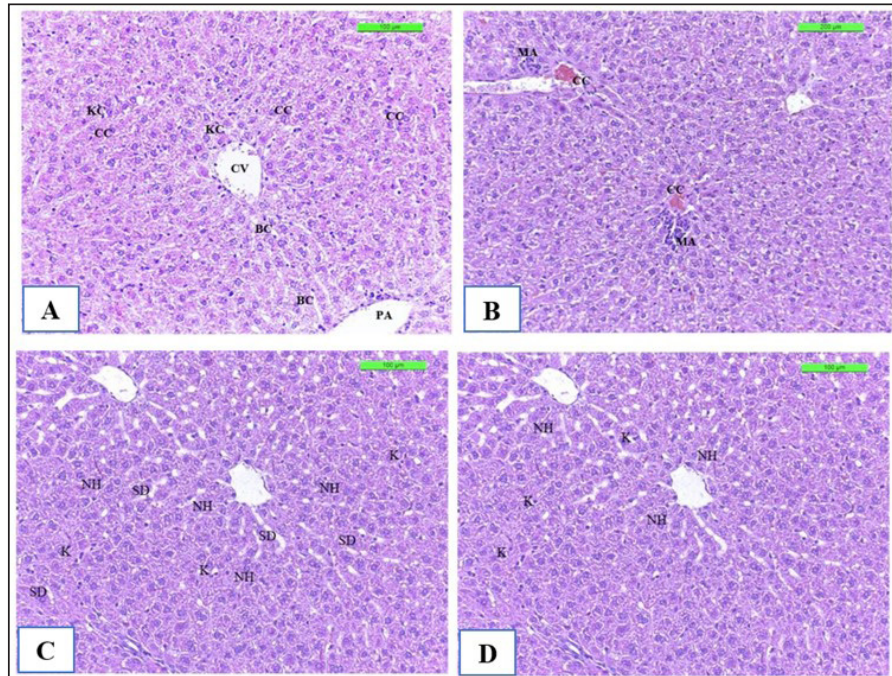
Fig. 11. The H&E staining sections of histopathological groups; the section (A) of Cont. − = G1 group shows villi (V), simple columnar epithelium (CE), lamina propria (LP), and goblet cells (GC) *X10*. The section (B) of Cont. + = G1 group indicating small intestine the villus diminishing (VD) and death of enterocytes (DE), and cellular infiltration (CI) detected among circular muscular fibers and irregular crypt (IC) structures *X10*. Section (C) of appearance small intestine expressions, the villi diminishing (VD), increased number of goblet cells (GC), and intestinal epithelial cells disordered (ED) *X20*. WKLMAgs = G3 group section (D) of *LCFPs* = G4 group demonstrates the normal structure of the small intestine with long columnar surface epithelial cells (CE) *X5*.

deficit and partial IgA + IgG subclass deficiency. Similarly, the clinical effectiveness and tolerance of preventive treatment with the oral immunomodulator bacterial extract OM85-BV or benzathine penicillin G in avoiding recurrent infections in symptomatic individuals have been studied. Wherever the level of IgG3 increased significantly on day 14 after the poster dose and on day 28 in positive control after a challenge with attenuated bacteria as a result, the presence of sufficient IgG3 isotypes against bacteria vaccinated with *LCFPs* and *WKLMAgs* groups may be enough to enhance bacterial clearance, while the reduced significant level of IgG3 in *WKLMAgs* and *LCFPs* after challenge at day 28 was reported by Nabonee *et al.* (2023) that the immunization-mediated humoral immune response can play a vital role in immunity for bacteria after challenge. Together with Wang *et al.* (2023) immune cells successfully killed invasive bacteria by directly capturing IgG-coated pathogens through several FcγRs.

Howbeit, the perivascular space's macrophages were drawn from the monocytes in circulation. The astrocytes and oligodendrocytes have a limited repertoire of responses to injury in the CNS (Fig. 8B),

which is similar to what was reported by Engelen-Lee who has shown that the inflammation within the ventricles, along with abscess formation and extensive efferocytosis, has been proposed as a mechanism potentially utilized by LM for facilitating cell-to-cell transmission (Engelen-Lee *et al.*, 2018). Likewise, the most frequently expressed immunomodulatory signals shortly after LM infection were the IL-1β family members as in Figure 6 and the chemokine CCl-2, which both are implicated in Th1 responses. These genes were found to be elevated in comparison with negative control, which appeared normal structure of tissue (Remuzgo-MartÍnez *et al.*, 2013). According to Lassmann et al.'s (2001) research, vaccination with CFA/PTX in the absence of CNS autoantigen can cause a modest inflammatory response in the brain of wild-type mice.. Ma *et al.* (2020) described that in spleen and liver, histology of positive control triggering necrosis of lymphocytes in the white pulp and congestion in the spleen with microgranuloma in the liver were observed. In LM-infected mice, the most frequently invaded organs are the spleen and liver in addition to the brain (Ma *et al.*, 2020). Shihab and Ibrahim (2021) stated that the spleen histology
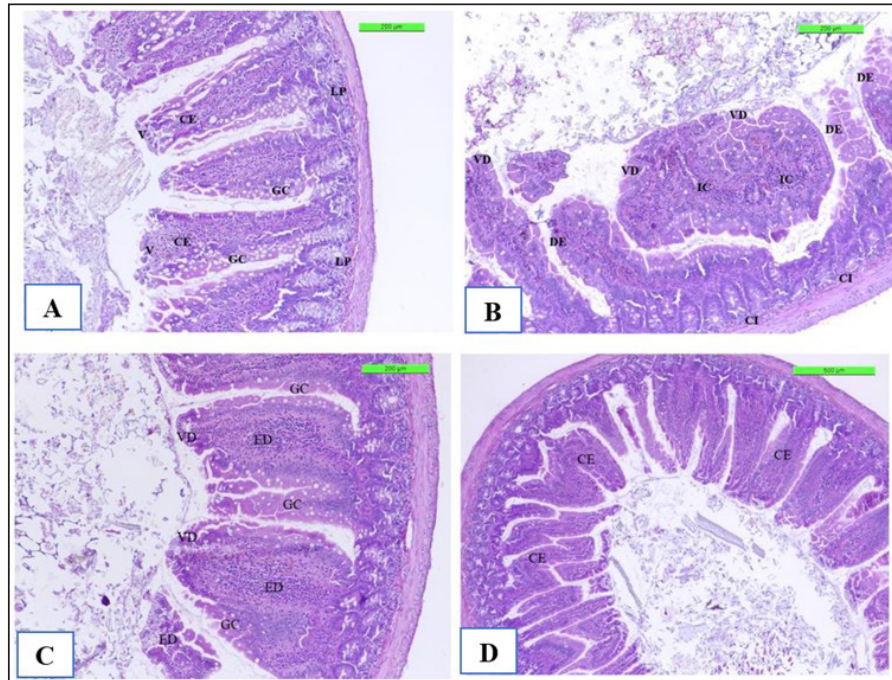
Fig. 5. The pre- and post-challenge statistically substantial CXCL2 between the groups exposed significant variance $p < 0.009$ and $p < 0.001$ at day 21 in pre-challenge groups of animals G3 and G4, respectively, as well as at day 28 in the post-challenge groups G2–G4 with virulent LM compared with the control negative G1 at days 21 and 35. No significant difference between G3 and G4 at 21 or 35 days, together with day 0 between all groups (Cont. − = G1, Cont. − = G2, *WKLMAgs* = G3, and *LCFPs* = G4). Two-way ANOVA was used to evaluate significant changes in mean total cell (*$p < 0.05$, **$p < 0.01$, and ***$p < 0.001$; ns: not significant).

showed that the *WKLMAgs* and *LCFPs* groups caused less damage to organs and lymphoproliferative than the negative group. During that time, the cytoplasm of hepatocyte exhibited a subtle stain, and the boundaries of the cells were not clearly defined in Figure 10B, which is similar to what was shown by Adeshina and Emikpe (2020) where they referred that the rat exposed to *Listeria* infection exposed modest zonal degeneration of hepatocytes was detected in the liver. This result was paralleling in the previous study by Bastos *et al.* (2020). The immunization with *WKLMAgs* and *LCFPs* groups caused less damage to organs than the negative group and protection of the liver tissue (Bastos *et al.*, 2020). Furthermore, animals inoculated with the recombinant BCG vaccinations had smaller and fewer liver, spleen, and lung lesions upon necropsy (Horwitz *et al.*, 2000). Reis *et al.* (2008) indicated in their study that 60 days following an infectious challenge, mice immunized with rPb27 exhibited a notable level of protection in the lungs (93%), liver (93%), and spleen (10%). At the same time, Abdelfattah *et al.* (2023) and Nikitas *et al.* (2011) reported that Gram-positive LM can penetrate intestinal epithelium and cause mild to severe

enteritis. It also causes systemic infection in positive control and is associated with focal mononuclear inflammatory cells in the submucosal layer and among intestinal crypts (Nikitas *et al.*, 2011; Abdelfattah *et al.*, 2023) compared to negative control in Figure 11A. Parallel to Ahmed *et al.* (2022), the intestine in the *WKLMAgs* and *LCFPs* groups provides an immune booster with a long-acting immunological impact and fewer alterations in the gut following a challenge dosage. Specifically in the previous study, following a challenge with virulent *Clostridium perfringens*, hens inoculated with the recombinant attenuated *Salmonella enterica serovar Typhimurium* vaccine exhibited less intestinal mucosal pathology (Zekarias *et al.*, 2008).

Conclusions
In summary, based on the results obtained from this work, the *WKLMAgs* and *LCFPs* conferred increased efficacy against challenge doses of virulent LM *in vivo* in comparison with positive control. The observed better antibody responses by *WKLMAgs* and *LCFPs* suggest a greater preservation of natural protein (Ag) conformations than expected, so further studies should

be assumed to clarify the immune parameters that lead to augmented protectivity.

References
Abdelfattah, A., Samir, R. and Amin, H.M. 2023. Production of highly immunogenic and safe Triton X-100 produced bacterial ghost vaccine against *Shigella* flexneri 2b serotype. Gut Pathog. 15(1), 41.

Adeshina, I. and Emikpe, B.O. 2020. Pathogenicity, haematology and pathology of *Listeria* monocytogenes in rat. Comp. Clin. Pathol. 29(2), 511–515.

Ahmed, S., Nemr, W.A., Ahmed Mohamed, W.A., Mohamed, A.M. and El-Fatah Mahmoud, M.A. 2022. Evaluation of room temperature (30 C to 35 C) lyophilized vaccine with radio inactivated Mannheimia haemolytica whole cells isolated from infected sheep. Vet. World 15(5), 1261–1268.

Al-Alwan, L.A., Chang, Y., Mogas, A., Halayko, A.J., Baglole, C.J., Martin, J.G., Rousseau, S., Eidelman, D.H. and Hamid, Q. 2013. Differential roles of CXCL2 and CXCL3 and their receptors in regulating normal and asthmatic airway smooth muscle cell migration. J. Immun. 191(5), 2731–2741.

Alao, M.A., Maroushek, S., Slusher, T.M., Joseph, A. and Gbadero, D.A. 2019. A case report of listeria monocytogenes meningitis in a child with hyper-igm syndrome in a resource-limited setting. Glob Pediatr Health 6, 2333794X19835571.

Al-Sabawi, B.H., Sadoon, H.S. and Saeed, M.G. 2023. Histochemical study of the hepatic metacestodes in sheep infected with hydatidosis. Iraqi J. Vet. Med. 37(1), 45–51.

Andersen, P. and Doherty, T.M. 2005. The success and failure of BCG—implications for a novel tuberculosis vaccine. Nat. Rev. Microbiol. 3(8), 656–662.

Arijo, S., Balebona, C., Martinez-Manzanares, E. and Moriñigo, M.A. 2004. Immune response of gilt-head seabream (*Sparus aurata*) to antigens from *Photobacterium damselae* subsp. piscicida. Fish Shellfish Immunol. 16, 65–70.

Baggiolini, M. 2001. Chemokines in pathology and medicine. J. Intern. Med. 250(2), 91–104.

Bahramian, E., Shahhosseiny, M.H., Shakib, P., Zolfaghari, M.R. and Ahmadi, S. 2023. Evaluation of hly-A and 16S rRNA genes for detection of *Listeria* monocytogenes in raw milk sample. J. Chronic Dis. 2023, 186–190.

Baker, C.J., Paoletti, L.C., Rench, M.A., Guttormsen, H.K., Edwards, M.S. and Kasper, D.L. 2004. Immune response of healthy women to 2 different group B streptococcal type V capsular polysaccharide-protein conjugate vaccines. J. Infect. Dis. 189(6), 1103–1112.

Bastos, D.S.S., Miranda, B.M., Martins, T.V.F., Ervilha, L.O.G., Souza, A.C.F., de Oliveira Emerick, S., da Silva, A.C., Novaes, R.D., Neves, M.M., Santos, E.C. and de Oliveira, L.L. 2020. Lipophosphoglycan-3 recombinant protein vaccine controls hepatic parasitism and prevents tissue damage in mice infected by *Leishmania infantum* chagasi. Biomed. pharmacother. 126, 110097.

Beikzadeh, B. 2024. Immunoinformatics design of novel multi-epitope vaccine against *Trueperella pyogenes* using collagen adhesion protein, fimbriae, and pyolysin. Arch. Microbiol. 206(3), 90.

Belperio, J.A., Keane, M.P., Burdick, M.D., Lynch, J.P., Xue, Y.Y., Berlin, A., Ross, D.J., Kunkel, S.L., Charo, I.F. and Strieter, R.M. 2001. Critical role for the chemokine MCP-1/CCR2 in the pathogenesis of bronchiolitis obliterans syndrome. J. Clin. Investig. 108(4), 547–556.

Bent, R., Moll, L., Grabbe, S. and Bros, M. 2018. Interleukin-1 beta—a friend or foe in malignancies? Int. J. Mol. Sci. 19(8), 2155.

Biondo, C., Mancuso, G., Midiri, A., Signorino, G., Domina, M., Lanza Cariccio, V., Mohammadi, N., Venza, M., Venza, I., Teti, G. and Beninati, C. 2014. The interleukin-1β/CXCL1/2/neutrophil axis mediates host protection against group B streptococcal infection. Infect. Immun. 82(11), 4508–4517.

Boes, M. 2000. Role of natural and immune IgM antibodies in immune responses. Mol. Immunol. 37(18), 1141–1149.

Boyle, M.J., Reiling, L., Feng, G., Langer, C., Osier, F.H., Aspeling-Jones, H., Cheng, Y.S., Stubbs, J., Tetteh, K.K., Conway, D.J. and McCarthy, J.S. 2015. Human antibodies fix complement to inhibit *Plasmodium falciparum* invasion of erythrocytes

and are associated with protection against malaria. Immunity 42(3), 580–590.

Bradford, M.M. 1976. A rapid and sensitive method for the quantitation of microgram quantities of protein utilizing the principle of protein-dye binding. Anal. Biochem. 72(1–2), 248–254.

Capita, R., Alonso-Calleja, C., Prieto, M., del Camino García-Fernández, M. and Moreno, B. 2001. Comparison of PALCAM and modified Oxford plating media for isolation of *Listeria* species in poultry meat following UVM II or Fraser secondary enrichment broths. Food Microbiol. 18(5), 555–563.

Cong, Z., Xiong, Y., Lyu, L., Fu, B., Guo, D., Sha, Z., Yang, B. and Wu, H. 2024. The relationship between *Listeria* infections and host immune responses: listeriolysin O as a potential target. Biomed. Pharmacother. 171, 116129.

Cowley, M.J., Weinberg, A., Zammit, N.W., Walters, S.N., Hawthorne, W.J., Loudovaris, T., Thomas, H., Kay, T., Gunton, J.E., Alexander, S.I. and Kaplan, W. 2012. Human islets express a marked proinflammatory molecular signature prior to transplantation. Cell Transplant. 21(9), 2063–2078.

Crowley, E., Bird, P., Fisher, K., Goetz, K., Boyle, M., Benzinger, Jr, M.J., Juenger, M., Agin, J., Goins, D. and Johnson, R.L. 2012. Evaluation of the VITEK 2 gram positive (GP) microbial identification test card: collaborative study. J. AOAC Int. 95(5), 425–1432.

Damelang, T., Rogerson, S.J., Kent, S.J. and Chung, A.W. 2019. Role of IgG3 in infectious diseases. Trends Immunol. 40(3),197–211.

Dhama, K., Karthik, K., Tiwari, R., Shabbir, M.Z., Barbuddhe, S., Malik, S.V.S. and Singh, R.K. 2015. Listeriosis in animals, its public health significance (food-borne zoonosis) and advances in diagnosis and control: a comprehensive review. Vet. Quart. 35(4), 211–235.

Engelen-Lee, J.Y., Koopmans, M.M., Brouwer, M.C., Aronica, E. and van de Beek, D. 2018. Histopathology of *Listeria* meningitis. J. Neuropathol. Exp. Neurol. 77(10), 950–957.

Fatsi, P.S.K., Kawai, K., Asmah, R., Oppong, B.B., Appiah, E.K., Hashem, S., Addo, A., Kusorgbor, J.K., Magna, E.K., Obeng, A.K. and Quansah, L. 2024. Immunomodulation and humoral immune response in teleost immunized with aeromonas-derived antigenic extracellular bioactive molecules. Indian J. Microbiol. 2024, 1–13.

Feltham, L., Moran, J., Goldrick, M., Lord, E., Spiller, D.G., Cavet, J.S., Muldoon, M., Roberts, I.S. and Paszek, P. 2024. Bacterial aggregation facilitates internalin-mediated invasion of *Listeria* monocytogenes. Front Cell Infect. Microbiol. 14, 1411124.

Fraussen, J. 2022. IgM responses following SARS-CoV-2 vaccination: insights into protective and pre-existing immunity. E. Bio. Med. 2022, 77.

Genel, F. and Kutukculer, N. 2003. Prospective, randomized comparison of OM-85 BV and a prophylactic antibiotic in children with recurrent infections and immunoglobulin A and/or G subclass deficiency. Curr. Ther. Res. 64(8), 600–615.

Gmeiner, A., Njage, P.M.K., Hansen, L.T., Aarestrup, F.M. and Leekitcharoenphon, P. 2024. Predicting *Listeria* monocytogenes virulence potential using whole genome sequencing and machine learning. Int. J. Food Microbiol. 410, 110491.

Guo, H.L., Shi, F.D., Zhou, Q., Liu, Q.Y., Wang, Y.X., Song, Y., Wu, Z.S., Shi, Y.H., Zhang, L., Xu, K.Z. and Song, G.D. 2021. Interleukin-1β protection against experimental sepsis in mice. Inflammation 44, 358–370.

Gupta, S. and Gupta, A. 2017. Selective IgM deficiency—an underestimated primary immunodeficiency. Front Immunol. 8, 1056.

Halbedel, S., Wilking, H., Holzer, A., Kleta, S., Fischer, M.A., Lüth, S., Pietzka, A., Huhulescu, S., Lachmann, R., Krings, A. and Ruppitsch, W. 2020. Large nationwide outbreak of invasive listeriosis associated with blood sausage, Germany, 2018–2019. Emerg. Infect. Dis. 26(7), 1456.

Hardy, J., Kirkendoll, B., Zhao, H., Pisani, L., Luong, R., Switzer, A., McConnell, M.V. and Contag, C.H. 2012. Infection of pregnant mice with *Listeria* monocytogenes induces fetal bradycardia. Pediatr. Res. 71(5), 539–545.

Horwitz, M.A., Harth, G., Dillon, B.J. and Masleša-Galić, S. 2000. Recombinant *Bacillus* Calmette–Guérin (BCG) vaccines expressing the *Mycobacterium tuberculosis* 30-kDa major secretory protein induce greater protective immunity against tuberculosis than conventional BCG vaccines in a highly susceptible animal model. Proc. Natl. Acad. Sci. U. S. A. 97(25), 13853–13858.

Imhof, D., Pownall, W., Hänggeli, K.P.A., Monney, C., Román, L.R.S., Ortega-Mora, L.M., Forterre, F., Oevermann, A. and Hemphill, A. 2023. Immunization with a multivalent *Listeria* monocytogenes vaccine leads to a strong reduction in vertical transmission and cerebral parasite burden in pregnant and non-pregnant mice infected with *Neospora caninum*. Vaccines 11(1), 156.

Jibo, G.G., Raji, Y.E., Salawudeen, A., Amin-Nordin, S., Mansor, R. and Jamaluddin, T.Z.M.T. 2022. A systematic review and meta-analysis of the prevalence of *Listeria* monocytogenes in South-East Asia; a one-health approach of human-animal-food-environment. One Health 15, 100417.

Kajikawa, A., Masuda, K., Katoh, M. and Igimi, S. 2010. Adjuvant effects for oral immunization provided by recombinant *Lactobacillus casei*

secreting biologically active murine interleukin-1β. Clin. Vaccine Immunol. 17(1), 43–48.

Kana, I.H., Singh, S.K., Garcia-Senosiain, A., Dodoo, D., Singh, S., Adu, B. and Theisen, M. 2019. Breadth of functional antibodies is associated with *Plasmodium falciparum* merozoite phagocytosis and protection against febrile malaria. J. Infect. Dis. 220(2), 275–284.

Kim, S.H., Chon, J.W., Jeong, H.W., Song, K.Y., Kim, D.H., Bae, D., Kim, H. and Seo, K.H. 2023. Identification and phylogenetic analysis of *Enterococcus* isolates using MALDI-TOF MS and VITEK 2. AMB Expr. 13(1), 21.

Kono, M., Iyo, T., Murakami, D., Sakatani, H., Nanushaj, D. and Hotomi, M. 2023. Maternal immunization with pneumococcal surface protein A provides the immune memories of offspring against pneumococcal infection. Front Cell Infect. Microbiol. 13, 1059603.

Lachmann, R., Halbedel, S., Lüth, S., Holzer, A., Adler, M., Pietzka, A., Al Dahouk, S., Stark, K., Flieger, A., Kleta, S. and Wilking, H. 2022. Invasive listeriosis outbreaks and salmon products: a genomic, epidemiological study. Emerg. Microbes Infect. 11(1), 1308–1315.

Lassmann, S., Kincaid, C., Asensio, V.C. and Campbell, I.L. 2001. Induction of type 1 immune pathology in the brain following immunization without central nervous system autoantigen in transgenic mice with astrocyte-targeted expression of IL-12. J. Immun. 167(9), 5485–5493.

Lentini, G., De Gaetano, G.V., Famà, A., Galbo, R., Coppolino, F., Mancuso, G., Teti, G. and Beninati, C. 2022. Neutrophils discriminate live from dead bacteria by integrating signals initiated by Fprs and TLRs. EMBO J. 41(5), e109386.

Luo, Z., Chang, G., Liu, Y., Ni, K., Zhou, T., Lv, X., Yu, J., Bai, J. and Wang, X. 2022. Inactivation of suspended cells and biofilms of the gram-negative bacteria by electron beam irradiation and possible mechanisms of action. LWT 172, 114171.

Ma, J., Xie, M., Wang, S., Ji, Q., Guo, L., Wang, Z., Qiu, J., Xu, D. and Liu, Q. 2020. Immunological evaluation of virulence-deficient *Listeria* monocytogenes strains in C57BL/6 mice. Microb. Pathog. 148, 104448.

Mahmud, J., Muranyi, P., Salmieri, S. and Lacroix, M. 2023. Optimization of a natural antimicrobial formulation against potential meat spoilage bacteria and food-borne pathogens: mixture design methodology and predictive modeling. Microb. Pathog. 176, 106000.

Manqele, A., Gcebe, N., Pierneef, R.E., Moerane, R. and Adesiyun, A.A. 2023. Identification of *Listeria* species and multilocus variable-number tandem repeat analysis (MLVA) typing of *Listeria innocua* and *Listeria* monocytogenes isolates from cattle farms and beef and beef-based products from retail outlets in Mpumalanga and north west provinces, South Africa. Pathogens 12(1), 147.

Maudet, C., Levallois, S., Disson, O. and Lecuit, M. 2021. Innate immune responses to *Listeria* in vivo. Curr. Opin. Microbiol. 59, 95–101.

Mehrannia, L., Khalilzadeh, B., Rahbarghazi, R., Milani, M., Saydan Kanberoglu, G., Yousefi, H. and Erk, N. 2023. Electrochemical biosensors as a novel platform in the identification of listeriosis infection. Biosensors 13(2), 216.

Meng, F., Zhu, T., Yao, H., Ling, Z., Feng, Y., Li, G., Li, J., Sun, X., Chen, J., Meng, C. and Jiao, X.A. 2020. A cross-protective vaccine against 4b and 1/2b *Listeria* monocytogenes. Front. Microbiol. 11, 569544.

Mohamed, A.H., Yaseen, S.S., Azeez, A.A. and Abass, K.S. 2022. The annual incidence of *Listeria* monocytogenes infection among pregnant women with abortion and premature birth effects in Kirkuk city, Iraq. Rev. Latinoam. Hipertens. 17(1), 1–7.

Mushtaq, M., Sadique, U., Said, F., Shah, M., Amanullah, H. and Anwer, F. 2022. Immunomodulatory and hepato-protective role of water based supplemented *Bacillus clausii* in broiler chicks. J. Saudi Soc. Agric. Sci. 21(2), 108–113.

Nabonee, M.A., Rahman, A., Mishu, N.J., Dola, N.Z. and Shamsuzzaman, S.M. 2023. Immunization with formaldehyde inactivated whole cell vaccine against multidrug resistant *Pseudomonas aeruginosa* produces protective IgG antibodies in mice model. Arch. Microbiol. Immunol. 7, 230–235.

Napodano, C., Marino, M., Stefanile, A., Pocino, K., Scatena, R., Gulli, F., Rapaccini, G.L., Delli Noci, S., Capozio, G., Rigante, D. and Basile, U. 2021. Immunological role of IgG subclasses. Immunol. Investig. 50(4), 427–444.

Nikitas, G., Deschamps, C., Disson, O., Niault, T., Cossart, P. and Lecuit, M. 2011. Transcytosis of *Listeria* monocytogenes across the intestinal barrier upon specific targeting of goblet cell accessible E-cadherin. J. Exp. Med. 208(11), 2263–2277.

Noomy, B.S., Anwar, S.A. and Salih, S.M. 2021. Detection of *Listeria* monocytogenes in raw milk and aborted cow cases at Salahudeen province. Iraqi J. Agric. Sci. 52(2), 315–321.

Oeuvray, C., Bouharoun-Tayoun, H., Gras-Masse, H., Bottius, E., Kaidoh, T., Aikawa, M., Filgueira, M.C., Tartar, A. and Druilhe, P. 1994. Merozoite surface protein-3: a malaria protein inducing antibodies that promote *Plasmodium falciparum* killing by cooperation with blood monocytes. Blood 84,1594–1602.

Omer, E., Elfehid, M., Alwazan, A., Alouffi, A.S., Alshammari, F.A., Eldesoukey, I. and Sultan, K. 2022. Molecular detection of *Anaplasma marginale* in Arabian camels (*Camelus dromedarius*) in Riyadh, Saudi Arabia. J. Saudi Soc. Agric. Sci. 21(2), 73–76.

Patas, K., Mavridis, T., Psarra, K., Papadopoulos, V.E., Mandilara, G., Tsirogianni, A., Vassilopoulou, S. and Chatzipanagiotou, S. 2020. Neurolisteriosis in a previously asymptomatic patient with serum IgM deficiency: a case report. BMC Neurol. 20, 1–6.

Prantner, D., Darville, T., Sikes, J.D., Andrews Jr, C.W., Brade, H., Rank, R.G. and Nagarajan, U.M. 2009. Critical role for interleukin-1β (IL-1β) during *Chlamydia muridarum* genital infection and bacterial replication-independent secretion of IL-1β in mouse macrophages. Infect. Immun. 77(12), 5334–5346.

Pulpipat, T., Maekawa, S., Wang, P.C. and Chen, S.C. 2020. Immune responses and protective efficacy of a formalin-killed *Francisella noatunensis* subsp. orientalis vaccine evaluated through intraperitoneal and immersion challenge methods in *Oreochromis niloticus*. Vaccines 8(2), 163.

Razzak, L.A., Hisham, N.A., Abu Darwish, M.M. and Sheikh, H. 2024. Efficacy of vaccine from whole killed *Vibrio alginolyticus* cells on the immune response of white shrimp (*Litopenaeus vannamei*). Iraqi J. Vet. Med. 38(1), 37–44.

Reis, B.S., Fernandes, V.C., Martins, E.M.N., Serakides, R. and Goes, A.M. 2008. Protective immunity induced by rPb27 of *Paracoccidioides brasiliensis*. Vaccine 26(43), 5461–5469.

Remuzgo-Martĺnez, S., Pilares-Ortega, L., Icardo, J.M., ValdizÁn, E.M., Vargas, V.I., Pazos, A. and Ramos-Vivas, J. 2013. Microglial activation and expression of immune-related genes in a rat ex vivo nervous system model after infection with *Listeria* monocytogenes. Glia 61(4), 611–622.

Sahoo, M., Ceballos-Olvera, I., del Barrio, L. and Re, F. 2011. Role of the inflammasome, IL-1β, and IL-18 in bacterial infections. Sci. World J. 11(1), 2037–2050.

Salinas-Carmona, M.C. and Pérez-Rivera, I. 2004. Humoral immunity through immunoglobulin M protects mice from an experimental actinomycetoma infection by *Nocardia brasiliensis*. Infect. Immun. 72(10), 5597–5604.

Sarkar, M.S.I., Hossain, M.S., Hasan, M.M., Khan, M., Al Islam, A. and Kamal, M. 2024. Temporal variation in quality characteristics of nutritional constituents and bacterial community during dry salt-fermentation of hilsa (*Tenualosa ilisha*). Food Prod. Process Nutr. 6(1), 48.

Schaut, R.G., Boggiatto, P.M., Loving, C.L. and Sharma, V.K. 2019. Cellular and mucosal immune responses following vaccination with inactivated mutant of *Escherichia coli* O157: H7. Sci. Rep. 9(1), 6401.

Shalaby, A., Ismail, M.M. and El-Sharkawy, H. 2022. Isolation, identification, and genetic characterization of antibiotic resistance of *Salmonella* species isolated from chicken farms. J. Trop. Med. 2022(1), 6065831.

Shihab, T.J. and Ibrahim, Z.I. 2021. Immunohistochemical and pathological changes in BALB/c mice immunized with whole sonicated *Listeria* monocytogenes antigens and the effect of probiotics. Iraqi J. Vet. Med. 35, 79–85.

Shin, A.R., Lee, K.S., Lee, J.S., Kim, S.Y., Song, C.H., Jung, S.B., Yang, C.S., Jo, E.K., Park, J.K., Paik, T.H. and Kim, H.J. 2006. *Mycobacterium tuberculosis* HBHA protein reacts strongly with the serum immunoglobulin M of tuberculosis patients. Clin. Vaccine Immunol. 13(8), 869–875.

Silvério, D., Gonçalves, R., Appelberg, R. and Saraiva, M. 2021. Advances on the role and applications of interleukin-1 in tuberculosis. MBio 12(6), e03134–21.

Sunden, Y., Yano, S., Ishida, S., Ochiai, K. and Umemura, T. 2010. Intracerebral vaccination suppresses the spread of rabies virus in the mouse brain. Microbes Infect. 12(14–15), 1163–1169.

Tahtinen, S., Tong, A.J., Himmels, P., Oh, J., Paler-Martinez, A., Kim, L., Wichner, S., Oei, Y., McCarron, M.J., Freund, E.C. and Amir, Z.A. 2022. IL-1 and IL-1ra are key regulators of the inflammatory response to RNA vaccines. Nat. Immunol. 23(4), 532–542.

Théroude, C., Reverte, M., Heinonen, T., Ciarlo, E., Schrijver, I.T., Antonakos, N., Maillard, N., Pralong, F., Le Roy, D. and Roger, T. 2021. Trained immunity confers prolonged protection from listeriosis. Front. Immunol. 12, 723393.

Tsai, J.L., Priya, T.J., Hu, K.Y., Yan, H.Y., Shen, S.T. and Song, Y.L. 2014. Grouper interleukin-12, linked by an ancient disulfide-bond architecture, exhibits cytokine and chemokine activities. Fish Shellfish Immunol. 36(1), 27–37.

Tucci, P., Portela, M., Chetto, C.R., González-Sapienza, G. and Marin, M. 2020. Integrative proteomic and glycoproteomic profiling of *Mycobacterium tuberculosis* culture filtrate. PLoS One 15(3), e0221837.

Van Den Eeckhout, B., Van Hoecke, L., Burg, E., Van Lint, S., Peelman, F., Kley, N., Uzé, G., Saelens, X., Tavernier, J. and Gerlo, S. 2020. Specific targeting of IL-1β activity to CD8+ T cells allows for safe use as a vaccine adjuvant. NPJ Vaccines 5(1), 1–17.

Vernel-Pauillac, F., Murray, G.L., Adler, B., Boneca, I.G. and Werts, C. 2021. Anti-Leptospira immunoglobulin profiling in mice reveals strain specific IgG and persistent IgM responses associated with virulence and renal colonization. PLoS Negl. Trop. Dis. 15(3), e0008970.

Vidarsson, G., Dekkers, G. and Rispens, T. 2014. IgG subclasses and allotypes: from structure to effector functions. Front. Immunol. 5, 520.

Wang, J., An, H., Ding, M., Liu, Y., Wang, S., Jin, Q., Wu, Q., Dong, H., Guo, Q., Tian, X. and Liu, J. 2023. Liver macrophages and sinusoidal endothelial

cells execute vaccine-elicited capture of invasive bacteria. Sci. Transl. Med. 15(727), eade0054.

Wang, Y., Qu, K., Lu, W., Zhao, P., Wang, Z., Cui, C., Liu, Y., Yang, M., Yu, Y. and Wang, L. 2022. Neutrophils recruited to immunization sites initiating vaccine-induced antibody responses by locally expressing BAFF. iScience 25(6), 104453.

Westcott, M.M., Blevins, M., Wierzba, T.F., Morse, A.E., White, K.R., Sanders, L.A. and Sanders, J.W. 2023. The immunogenicity and properties of a whole-cell ETEC vaccine inactivated with psoralen and UVA light in comparison to formalin. Microorganisms 11(8), 2040.

Zamuz, S., Munekata, P.E., Dzuvor, C.K., Zhang, W., Sant'Ana, A.S. and Lorenzo, J.M. 2021. The role of phenolic compounds against *Listeria* monocytogenes in food. A review. Trends Food Sci. Technol. 110, 385–392.

Zekarias, B., Mo, H. and Curtiss III, R. 2008. Recombinant attenuated *Salmonella enterica* serovar Typhimurium expressing the carboxy-terminal domain of alpha toxin from *Clostridium perfringens* induces protective responses against necrotic enteritis in chickens. Clin. Vaccine Immunol. 15(5), 805–816.

Zenewicz, L.A. and Shen, H. 2007. Innate and adaptive immune responses to *Listeria* monocytogenes: a short overview. Microbes Infect. 9(10), 1208–1215.

Zhou, H., Lu, X., Huang, J., Jordan, P., Ma, S., Xu, L., Hu, F., Gui, H., Zhao, H., Bai, Z. and Redmond, H.P. 2022. Induction of trained immunity protects neonatal mice against microbial sepsis by boosting both the inflammatory response and antimicrobial activity. J. Inflamm. Res.15, 3829–3845.